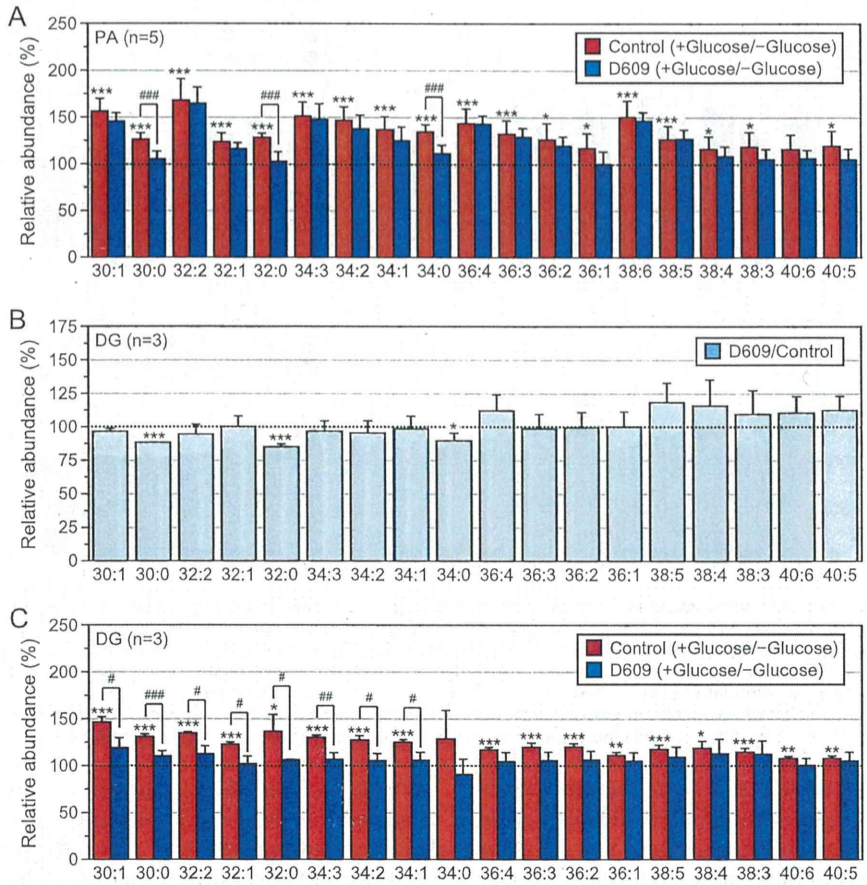

FIGURE 7. **Effect of D609 on high glucose-induced increases in PA and DG molecular species in C2C12 myoblasts.** *A*, the major PA molecular species in the glucose-unstimulated or glucose-stimulated cells treated with DMSO (control) or D609 were detected using the LC/ESI-MS method. The results are presented as the percentage of the value of PA molecular species in glucose-unstimulated cells treated with DMSO (control) or D609. D609 did not significantly affect the value of PA molecular species in glucose-unstimulated cells. The values are presented as the mean ± S.D. ($n = 5$). *, $p < 0.05$; ***, $p < 0.005$ (no stimulation *versus* glucose stimulation). ###, $p < 0.005$ (without D609 *versus* with D609). *B* and *C*, the major DG molecular species in the glucose-unstimulated or glucose-stimulated cells treated with DMSO (control) or D609 were detected using the ESI-MS method. *B*, comparison of +D609 *versus* −D609 in the absence of glucose. The results are presented as the percentage of the value of DG species in glucose-unstimulated cells treated with DMSO (control). The values are presented as the mean ± S.D. ($n = 3$). *, $p < 0.05$; ***, $p < 0.005$. *C*, comparison of +glucose *versus* −glucose in the absence or presence of D609. The results are presented as the percentage of the value of DG species in glucose-unstimulated cells treated with DMSO (control) or D609. D609 did not significantly affect the value of DG molecular species in glucose-unstimulated cells. The values are presented as the mean ± S.D. ($n = 3$). *, $p < 0.05$; **, $p < 0.01$; ***, $p < 0.005$ (no stimulation *versus* glucose stimulation). #, $p < 0.05$; ##, $p < 0.01$; ###, $p < 0.005$ (without D609 *versus* with D609).

stimulation statistically increased the PA mass and number of molecular species using the newly developed method (Fig. 1). The results indicate that our LC/ESI-MS method is a powerful tool for detecting even small changes in PA molecular species.

The suppression of DGKδ expression by RNA silencing decreased the high glucose-induced production of 30:0-, 32:0-, 34:1-, and 34:0-PA in C2C12 myoblasts (Fig. 2). Moreover, the levels of 30:1-, 30:0-, 32:1-, 32:0-, and 34:0-PA were substantially increased in a high glucose-dependent manner in C2C12 cells stably expressing DGKδ2 when compared with control cells (Fig. 4). Taken together, these results strongly suggest that DGKδ preferentially generates 30:0-, 32:0-, and 34:0-PA, which contain two saturated fatty acids, in the cells. The main fatty acid residues of these PA species were 14:0 and 16:0, 16:0 and 16:0, and 16:0 and 18:0, respectively (Table 1). These results suggest that DGKδ produces PA with an apparent preference for palmitic acid (16:0)-containing PA. Moreover, the suppression of DGKδ expression by siRNA-1 and -2 also decreased the high glucose-induced production of 34:1-PA (Fig. 2). The overexpression of DGKδ2 statistically increased the levels of 30:1- and 32:1-PA (Fig. 4). The DGKδ suppression also modestly attenuated 30:1- and 32:1-PA levels (Fig. 2), and the DGKδ2 overexpression slightly augmented 34:1-PA production (Fig. 4). Therefore, it is possible that this enzyme also generates 30:1-, 32:1-, and 34:1-PA, which contain one saturated and one monounsaturated fatty acid, in addition to 30:0-, 32:0-, and 34:0-PA. 30:1-, 32:1-, and 34:1-PA contain saturated fatty acids, 16:0 and 14:0, and monounsaturated fatty acids, 16:1 and 18:1 (Table 1). The DGKδ-siRNAs and DGKδ overexpression failed to statistically affect the amounts of high glucose-induced increases of 32:2-, 34:3-, 34:2-, 36:4-, 36:3-, 36:2-, and 38:6-PA (Figs. 2 and 4), implying that these PA species were generated by other DGK isozyme(s).

DGK is a member of the PI turnover pathway and initiates resynthesis of PI (18). This fact led us to believe that DGK isozymes, including DGKδ, also exhibit selectivity against 38:4 (18:0/20:4)-DG derived from PI turnover. Indeed, it was reported that DGKε preferentially phosphorylated DGs con-

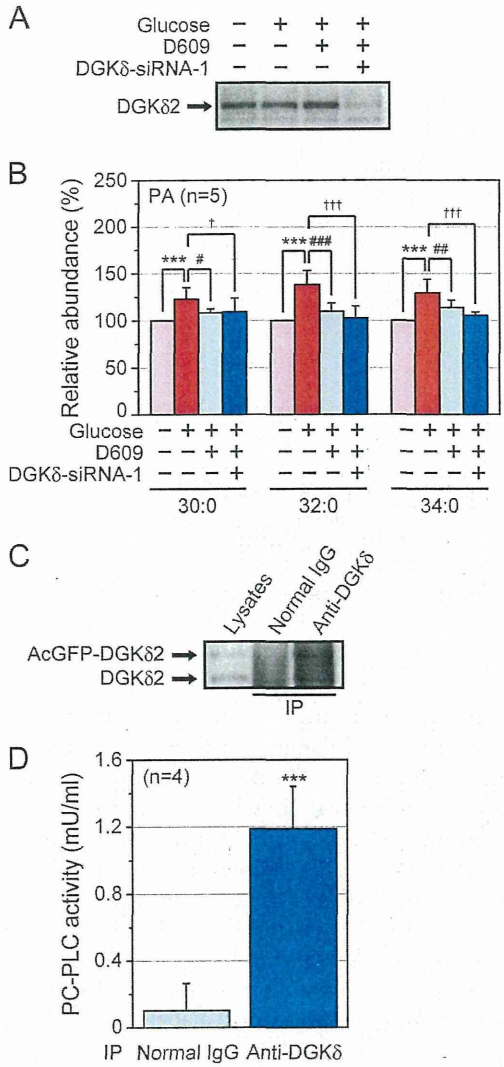

FIGURE 8. **Examination of the functional linkage between PC-PLC and DGKδ.** Effects of D609 and DGKδ-siRNA-1 on high glucose-induced increases of PA molecular species in C2C12 myoblasts were compared. *A*, the suppression of DGKδ2 expression by DGKδ-siRNA-1 was confirmed by Western blot analysis using the anti-DGKδ antibody. *B*, 30:0-, 32:0-, and 34:0-PA in the glucose-unstimulated or glucose-stimulated cells treated with DMSO (control), D609, or D609 and DGKδ-siRNA-1 were detected using the LC/ESI-MS method. The results are presented as the percentage of the value of PA molecular species in glucose-unstimulated cells. The values are presented as the mean ± S.D. ($n = 5$). ***, $p < 0.005$ (no stimulation *versus* glucose stimulation). #, $p < 0.05$; ##, $p < 0.01$; ###, $p < 0.005$ (without D609 *versus* with D609). †, $p < 0.05$; †††, $p < 0.005$ (control siRNA *versus* DGKδ-siRNA-1). *C* and *D*, co-immunoprecipitation of PC-PLC activity with DGKδ2. *C*, immunoprecipitation (*IP*) of DGKδ2 using the anti-DGKδ antibody was confirmed by Western blot analysis using the anti-DGKδ antibody. *D*, PC-PLC activity in the precipitates was measured using the Amplex Red® PC-PLC assay kit. The values are presented as the mean ± S.D. ($n = 4$). ***, $p < 0.005$. When the assay was performed in the absence of alkaline phosphatase, the activity was not detectable.

taining arachidonic acid (*e.g.* 38:4 (18:0/20:4)-DG) derived from PI turnover (7, 19, 20). However, high glucose stimulation did not increase the amount of 38:4-PA (Figs. 1 and 2), which mainly consisted of 18:0/20:4-PA (Table 1). Moreover, DGKδ-siRNAs and DGKδ2 overexpression failed to affect the amounts of 38:4-PA in response to high glucose stimulation (Figs. 2 and 4). These results indicate that DGKδ does not phosphorylate 38:4-DG derived from PI turnover in a glucose-dependent manner.

DGKδ did not exhibit selectivity against 16:0/16:0 (32:0)- or 16:0/18:1 (34:1)-DG *in vitro* (Fig. 5). Therefore, we hypothesized that DGKδ exerts substrate selectivity in C2C12 cells through accessing a DG pool containing 30:0-, 32:0-, and 34:0-DG, and not via its intrinsic preference. There are three DG supply pathways, *i.e.* 1) *de novo* synthesis including acetyl-CoA carboxylase (30, 31), 2) the PLD/PA phosphatase route (32), and 3) PC hydrolysis by PC-specific PLC (33). Treatment with the PC-PLC inhibitor D609, but not inhibitors of acetyl-CoA carboxylase and PLD, strongly inhibited the high glucose stimulation-responsive production of 30:0-, 32:0-, and 34:0-PA (Fig. 7*A*). Moreover, RNA silencing of DGKδ failed to further inhibit the glucose-dependent increases in 30:0-, 32:0-, and 34:0-PA in the presence of D609 (Fig. 8*B*). Furthermore, PC-PLC was co-immunoprecipitated with DGKδ2 (Fig. 8*D*). Taken together, these results strongly suggest that 30:0-, 32:0-, and 34:0-DG phosphorylated by DGKδ2 in response to acute high glucose exposure are generated, at least in part, by PC hydrolysis catalyzed by PC-PLC (Fig. 9).

The role of sphingomyelin synthase as a potential PC-PLC was indicated (36). We cannot rule out the possibility that DGKδ2 partly utilizes sphingomyelin synthase-dependent DG. However, it is likely that DGKδ2 phosphorylates DG species generated, at least in part, by PC-PLC because the co-immunoprecipitates with DGKδ2 contained PC-PLC activity.

The molecular identity of PC-PLC remains unclear (35). In this study, DGKδ was revealed to directly or indirectly associate with PC-PLC. With the pulldown of PC-PLC activity with DGKδ2, there may be an opportunity to identify the unidentified PC-PLC enzyme by proteomics approaches. Therefore, DGKδ2 may serve as a good tool to search for the PC-PLC molecule.

D609 attenuated high glucose-dependent increases in various C30-C34 DG species (Fig. 7*C*). However, D609 strongly inhibited only the high glucose stimulation-responsive production of 30:0-, 32:0-, and 34:0-PA (Fig. 7*A*). Intriguingly, this inhibitor statistically reduced the amounts of 30:0-, 32:0-, and 34:0-DG in the absence of high glucose (Fig. 7*B*). Therefore, it is likely that, in response to acute high glucose stimulation (5 min), DGKδ2 mainly utilizes these DG species supplied from the PC-PLC pathway in a high glucose-independent manner. Moreover, DGKδ2 can generate 30:1-, 32:1-, and 34:1-PA, in addition to 30:0-, 32:0-, and 34:0-PA. (Figs. 2 and 4). Although D609 moderately attenuated 30:1-, 32:1-, and 34:1-PA generation (Fig. 7*A*), this inhibitor did not affect the amounts of 30:1-, 32:1-, and 34:1-DG in the absence of high glucose stimulation (Fig. 7*B*). However, D609 substantially inhibited high glucose-dependent increases for 30:1-, 32:1-, and 34:1-DG (Fig. 7*C*). These results suggest that DGKδ2 can utilize 30:1-, 32:1-, and 34:1-DG that are supplied from the PC-PLC pathway in a high glucose-dependent manner.

Recently, Shulga *et al.* (37) and Lowe *et al.* (38) reported that DGKδ positively regulated lipid synthesis, including DG and PA, during adipocyte differentiation. However, unlike for acute high glucose stimulation, a significant preference against DG and PA was not found. The increases were, at least in part, a

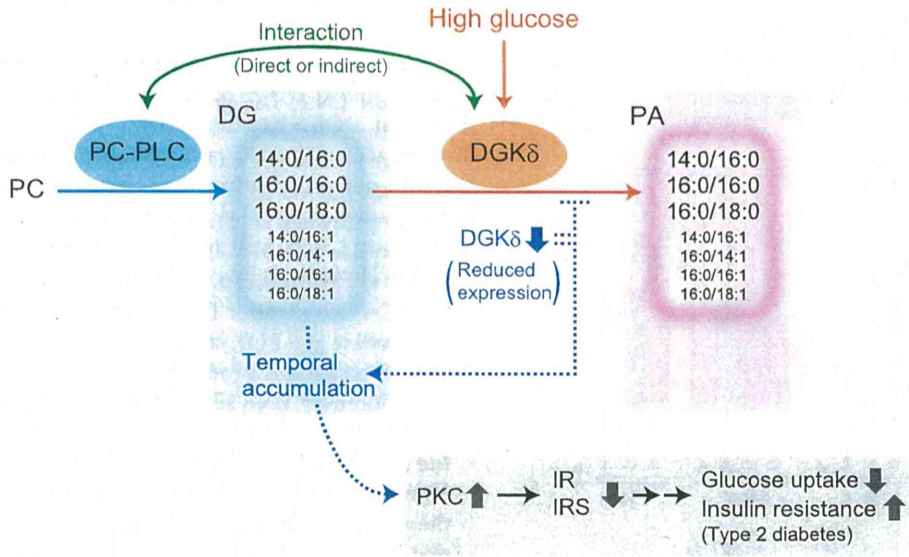

FIGURE 9. **Model for the metabolism pathway utilized by DGKδ.** *IR*, insulin receptor; *IRS*, insulin receptor substrate.

result of promoting the *de novo* synthesis of fatty acids. However, in this study, an inhibitor of acetyl-CoA carboxylase TOFA did not decrease glucose-stimulated PA production (Fig. 6*A*). Because differentiation is a long term event, the difference between acute high glucose stimulation in C2C12 myoblasts and adipocyte differentiation may be due to distinct supply pathways and/or fatty acid conversion during long term culture through the remodeling pathway (Lands' cycle) (39).

Chibalin *et al.* (15) previously reported that the transcription of DGKδ and the levels of DGKδ protein were also reduced in skeletal muscle from type II diabetes patients. Moreover, in DGKδ haploinsufficient mice ($DGK\delta^{+/-}$), the accumulation of DG, which was caused by decreases in total DGK activity and DGKδ protein levels in skeletal muscle, increased phosphorylation of PKCδ and suppressed protein expression of the insulin receptor and insulin receptor substrate-1 for insulin signaling, resulting in the aggravation of type II diabetes (15). Another study reported that the accumulation of DG molecular species with palmitic acid (16:0) is involved in insulin resistance (40). It is generally accepted that saturated fatty acids including palmitic acid induce insulin resistance (41–43). In this study, MS/MS analysis demonstrated that 30:0-, 30:1-, 32:0-, 32:1-, 34:0-, and 34:1-PA commonly contained palmitic acid (16:0), and suggests that DGKδ mainly consumes 30:0-, 30:1-, 32:0-, 32:1-, 34:0-, and 34:1-DG containing palmitic acid (16:0) supplied from the PC-PLC pathway for glucose uptake in skeletal muscle in a glucose-dependent manner. Acute high glucose- and DGKδ-dependent increases in 30:0-, 30:1-, 32:0-, 32:1-, 34:0-, and 34:1-PA were relatively minor changes (20–30% increases) when compared with the total amounts of each PA species (Figs. 1 and 2). DGKδ, which was temporarily activated within 5 min (16), showed a distinct punctate localization pattern in C2C12 cells (17). Therefore, a possible explanation of these findings is that these DGKδ-dependent minor changes of DG/PA species in temporally and spatially restricted regions play a role in modulating insulin signaling. However, further studies are required to elucidate the relationship between the specific DG species accumulation in type II diabetes patients and the PC-PLC-DGKδ pathway disclosed here.

In summary, the present study strongly suggests that DGKδ preferentially consumes palmitic acid (16:0)-containing DG species such as 30:0-, 30:1-, 32:0-, 32:1-, 34:0-, and 34:1-DG, but not arachidonic acid (20:4)-containing DG species derived from the phosphatidylinositol turnover, in glucose-stimulated C2C12 myoblasts (Fig. 9). Moreover, an unexpected linkage between PC-PLC and DGKδ emerged. The route "PC → PC-PLC → DG → DGK → PA" proposed here (Fig. 9) is a novel DG metabolic pathway. This new pathway is proposed to play an important role in glucose uptake in skeletal muscle and to be involved in the pathogenesis of type 2 diabetes.

REFERENCES

1. Zimmet, P., Alberti, K. G., and Shaw, J. (2001) Global and societal implications of the diabetes epidemic. *Nature* **414,** 782–787
2. Biddinger, S. B., and Kahn, C. R. (2006) From mice to men: insights into the insulin resistance syndromes. *Annu. Rev. Physiol.* **68,** 123–158
3. Kraegen, E. W., Saha, A. K., Preston, E., Wilks, D., Hoy, A. J., Cooney, G. J., and Ruderman, N. B. (2006) Increased malonyl-CoA and diacylglycerol content and reduced AMPK activity accompany insulin resistance induced by glucose infusion in muscle and liver of rats. *Am. J. Physiol. Endocrinol. Metab.* **290,** E471–E479
4. Goto, K., Hozumi, Y., and Kondo, H. (2006) Diacylglycerol, phosphatidic acid, and the converting enzyme, diacylglycerol kinase, in the nucleus. *Biochim. Biophys. Acta* **1761,** 535–541
5. Mérida, I., Avila-Flores, A., and Merino, E. (2008) Diacylglycerol kinases: at the hub of cell signalling. *Biochem. J.* **409,** 1–18
6. Sakane, F., Imai, S., Kai, M., Yasuda, S., and Kanoh, H. (2007) Diacylglycerol kinases: why so many of them? *Biochim. Biophys. Acta* **1771,** 793–806
7. Shulga, Y. V., Topham, M. K., and Epand, R. M. (2011) Regulation and functions of diacylglycerol kinases. *Chem. Rev.* **111,** 6186–6208
8. van Blitterswijk, W. J., and Houssa, B. (2000) Properties and functions of diacylglycerol kinases. *Cell. Signal.* **12,** 595–605
9. Sakai, H., and Sakane, F. (2012) Recent progress on type II diacylglycerol kinases: the physiological functions of diacylglycerol kinase δ, η and κ and their involvement in disease. *J. Biochem.* **152,** 397–406
10. Sakane, F., Imai, S., Kai, M., Yasuda, S., and Kanoh, H. (2008) Diacylglycerol kinases as emerging potential drug targets for a variety of diseases. *Curr. Drug Targets* **9,** 626–640

11. Sakane, F., Imai, S., Yamada, K., Murakami, T., Tsushima, S., and Kanoh, H. (2002) Alternative splicing of the human diacylglycerol kinase δ gene generates two isoforms differing in their expression patterns and in regulatory functions. *J. Biol. Chem.* **277,** 43519–43526
12. Murakami, T., Sakane, F., Imai, S., Houkin, K., and Kanoh, H. (2003) Identification and characterization of two splice variants of human diacylglycerol kinase η. *J. Biol. Chem.* **278,** 34364–34372
13. Sakane, F., Imai, S., Kai, M., Wada, I., and Kanoh, H. (1996) Molecular cloning of a novel diacylglycerol kinase isozyme with a pleckstrin homology domain and a C-terminal tail similar to those of the EPH family of protein tyrosine kinase. *J. Biol. Chem.* **271,** 8394–8401
14. DeFronzo, R. A., Jacot, E., Jequier, E., Maeder, E., Wahren, J., and Felber, J. P. (1981) The effect of insulin on the disposal of intravenous glucose: results from indirect calorimetry and hepatic and femoral venous catheterization. *Diabetes* **30,** 1000–1007
15. Chibalin, A. V., Leng, Y., Vieira, E., Krook, A., Björnholm, M., Long, Y. C., Kotova, O., Zhong, Z., Sakane, F., Steiler, T., Nylén, C., Wang, J., Laakso, M., Topham, M. K., Gilbert, M., Wallberg-Henriksson, H., and Zierath, J. R. (2008) Downregulation of diacylglycerol kinase δ contributes to hyperglycemia-induced insulin resistance. *Cell* **132,** 375–386
16. Miele, C., Paturzo, F., Teperino, R., Sakane, F., Fiory, F., Oriente, F., Ungaro, P., Valentino, R., Beguinot, F., and Formisano, P. (2007) Glucose regulates diacylglycerol intracellular levels and protein kinase C activity by modulating diacylglycerol-kinase subcellular localization. *J. Biol. Chem.* **282,** 31835–31843
17. Takeuchi, M., Sakiyama, S., Usuki, T., Sakai, H., and Sakane, F. (2012) Diacylglycerol kinase δ1 transiently translocates to the plasma membrane in response to high glucose. *Biochim. Biophys. Acta* **1823,** 2210–2216
18. Hodgkin, M. N., Pettitt, T. R., Martin, A., Michell, R. H., Pemberton, A. J., and Wakelam, M. J. (1998) Diacylglycerols and phosphatidates: which molecular species are intracellular messengers? *Trends Biochem. Sci.* **23,** 200–204
19. Rodriguez de Turco, E. B., Tang, W., Topham, M. K., Sakane, F., Marcheselli, V. L., Chen, C., Taketomi, A., Prescott, S. M., and Bazan, N. G. (2001) Diacylglycerol kinase ϵ regulates seizure susceptibility and long-term potentiation through arachidonoyl-inositol lipid signaling. *Proc. Natl. Acad. Sci. U.S.A.* **98,** 4740–4745
20. Tang, W., Bunting, M., Zimmerman, G. A., McIntyre, T. M., and Prescott, S. M. (1996) Molecular cloning of a novel human diacylglycerol kinase highly selective for arachidonate-containing substrates. *J. Biol. Chem.* **271,** 10237–10241
21. Mizuno, S., Sakai, H., Saito, M., Kado, S., and Sakane, F. (2012) Diacylglycerol kinase-dependent formation of phosphatidic acid molecular species during interleukin-2 activation in CTLL-2 T-lymphocytes. *FEBS Open Bio.* **2,** 267–272
22. Amtmann, E. (1996) The antiviral, antitumoural xanthate D609 is a competitive inhibitor of phosphatidylcholine-specific phospholipase C. *Drugs Exp. Clin. Res.* **22,** 287–294
23. Halvorson, D. L., and McCune, S. A. (1984) Inhibition of fatty acid synthesis in isolated adipocytes by 5-(tetradecyloxy)-2-furoic acid. *Lipids* **19,** 851–856
24. Pizer, E. S., Thupari, J., Han, W. F., Pinn, M. L., Chrest, F. J., Frehywot, G. L., Townsend, C. A., and Kuhajda, F. P. (2000) Malonyl-coenzyme-A is a potential mediator of cytotoxicity induced by fatty-acid synthase inhibition in human breast cancer cells and xenografts. *Cancer Res.* **60,** 213–218
25. Su, W., Yeku, O., Olepu, S., Genna, A., Park, J. S., Ren, H., Du, G., Gelb, M. H., Morris, A. J., and Frohman, M. A. (2009) 5-Fluoro-2-indolyl deschlorohalopemide (FIPI), a phospholipase D pharmacological inhibitor that alters cell spreading and inhibits chemotaxis. *Mol. Pharmacol.* **75,** 437–446
26. Bligh, E. G., and Dyer, W. J. (1959) A rapid method of total lipid extraction and purification. *Can. J. Biochem. Physiol.* **37,** 911–917
27. Sakai, H., Tanaka, Y., Tanaka, M., Ban, N., Yamada, K., Matsumura, Y., Watanabe, D., Sasaki, M., Kita, T., and Inagaki, N. (2007) ABCA2 deficiency results in abnormal sphingolipid metabolism in mouse brain. *J. Biol. Chem.* **282,** 19692–19699
28. Callender, H. L., Forrester, J. S., Ivanova, P., Preininger, A., Milne, S., and Brown, H. A. (2007) Quantification of diacylglycerol species from cellular extracts by electrospray ionization mass spectrometry using a linear regression algorithm. *Anal. Chem.* **79,** 263–272
29. Imai, S., Yasuda, S., Kai, M., Kanoh, H., and Sakane, F. (2009) Diacylglycerol kinase δ associates with receptor for activated C kinase 1, RACK1. *Biochim. Biophys. Acta* **1791,** 246–253
30. Craven, P. A., Davidson, C. M., and DeRubertis, F. R. (1990) Increase in diacylglycerol mass in isolated glomeruli by glucose from de novo synthesis of glycerolipids. *Diabetes* **39,** 667–674
31. Wolf, B. A., Easom, R. A., McDaniel, M. L., and Turk, J. (1990) Diacylglycerol synthesis *de novo* from glucose by pancreatic islets isolated from rats and humans. *J. Clin. Invest.* **85,** 482–490
32. Bandyopadhyay, G., Sajan, M. P., Kanoh, Y., Standaert, M. L., Quon, M. J., Reed, B. C., Dikic, I., and Farese, R. V. (2001) Glucose activates protein kinase C-ζ/λ through proline-rich tyrosine kinase-2, extracellular signal-regulated kinase, and phospholipase D: a novel mechanism for activating glucose transporter translocation. *J. Biol. Chem.* **276,** 35537–35545
33. Ramana, K. V., Friedrich, B., Tammali, R., West, M. B., Bhatnagar, A., and Srivastava, S. K. (2005) Requirement of aldose reductase for the hyperglycemic activation of protein kinase C and formation of diacylglycerol in vascular smooth muscle cells. *Diabetes* **54,** 818–829
34. Schütze, S., Berkovic, D., Tomsing, O., Unger, C., and Krönke, M. (1991) Tumor necrosis factor induces rapid production of 1′2′diacylglycerol by a phosphatidylcholine-specific phospholipase C. *J. Exp. Med.* **174,** 975–988
35. Adibhatla, R. M., Hatcher, J. F., and Gusain, A. (2012) Tricyclodecan-9-yl-xanthogenate (D609) mechanism of actions: a mini-review of literature. *Neurochem. Res.* **37,** 671–679
36. Luberto, C., and Hannun, Y. A. (1998) Sphingomyelin synthase, a potential regulator of intracellular levels of ceramide and diacylglycerol during SV40 transformation: Does sphingomyelin synthase account for the putative phosphatidylcholine-specific phospholipase C? *J. Biol. Chem.* **273,** 14550–14559
37. Shulga, Y. V., Loukov, D., Ivanova, P. T., Milne, S. B., Myers, D. S., Hatch, G. M., Umeh, G., Jalan, D., Fullerton, M. D., Steinberg, G. R., Topham, M. K., Brown, H. A., and Epand, R. M. (2013) Diacylglycerol kinase δ promotes lipogenesis. *Biochemistry* **52,** 7766–7776
38. Lowe, C. E., Zhang, Q., Dennis, R. J., Aubry, E. M., O'Rahilly, S., Wakelam, M. J., and Rochford, J. J. (2013) Knockdown of diacylglycerol kinase δ inhibits adipocyte differentiation and alters lipid synthesis. *Obesity* **21,** 1823–1829
39. Shindou, H., Hishikawa, D., Harayama, T., Yuki, K., and Shimizu, T. (2009) Recent progress on acyl CoA:lysophospholipid acyltransferase research. *J. Lipid Res.* **50,** (suppl.) S46–S51
40. Coll, T., Eyre, E., Rodríguez-Calvo, R., Palomer, X., Sánchez, R. M., Merlos, M., Laguna, J. C., and Vázquez-Carrera, M. (2008) Oleate reverses palmitate-induced insulin resistance and inflammation in skeletal muscle cells. *J. Biol. Chem.* **283,** 11107–11116
41. Hu, F. B., van Dam, R. M., and Liu, S. (2001) Diet and risk of Type II diabetes: the role of types of fat and carbohydrate. *Diabetologia* **44,** 805–817
42. Hunnicutt, J. W., Hardy, R. W., Williford, J., and McDonald, J. M. (1994) Saturated fatty acid-induced insulin resistance in rat adipocytes. *Diabetes* **43,** 540–545
43. Vessby, B., Uusitupa, M., Hermansen, K., Riccardi, G., Rivellese, A. A., Tapsell, L. C., Nälsén, C., Berglund, L., Louheranta, A., Rasmussen, B. M., Calvert, G. D., Maffetone, A., Pedersen, E., Gustafsson, I. B., Storlien, L. H., and KANWU Study (2001) Substituting dietary saturated for monounsaturated fat impairs insulin sensitivity in healthy men and women: the KANWU Study. *Diabetologia* **44,** 312–319

Signal Transduction:

Diacylglycerol Kinase δ Phosphorylates Phosphatidylcholine-specific Phospholipase C-dependent, Palmitic Acid-containing Diacylglycerol Species in Response to High Glucose Levels

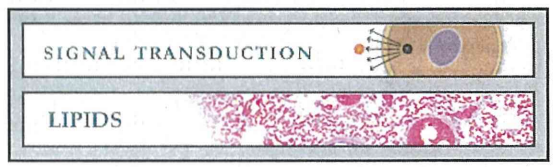

Hiromichi Sakai, Sayaka Kado, Akinobu Taketomi and Fumio Sakane

J. Biol. Chem. 2014, 289:26607-26617.
doi: 10.1074/jbc.M114.590950 originally published online August 11, 2014

Surg Today (2014) 44:2361–2365
DOI 10.1007/s00595-014-0949-6

CASE REPORT

Chondroma of the diaphragm mimicking a giant liver tumor with calcification: report of a case

Yoh Asahi · Toshiya Kamiyama · Kazuaki Nakanishi · Hideki Yokoo · Munenori Tahara · Akihiro Usui · Tohru Funakoshi · Masanori Sato · Ayami Sasaki · Yoshihiro Matsuno · Akinobu Taketomi · Satoru Todo

Received: 2 April 2013 / Accepted: 16 July 2013 / Published online: 17 June 2014

Abstract Extraskeletal chondroma is an unusual benign tumor, which rarely arises in the diaphragm. We report a case of chondroma of the diaphragm in a 31-year-old woman. Initially, a benign liver tumor with calcification was suspected, based on pre and intraoperative examination findings. Although parts of the tumor were contiguous with the diaphragm, its connections with the diaphragm were much narrower than its connection with the liver, which suggested a liver tumor. Pathological examination subsequently revealed that the chondroma was contiguous with the diaphragm and that there was a distinct border between the tumor and the liver; thus, the tumor was diagnosed as a chondroma of the diaphragm.

Keywords Chondroma · Extraskeletal · Diaphragmatic tumor · Calcification

Y. Asahi · T. Kamiyama (✉) · K. Nakanishi · H. Yokoo · M. Tahara · A. Usui · T. Funakoshi · M. Sato · A. Sasaki · A. Taketomi
Department of Gastroenterological Surgery I, Hokkaido University Graduate School of Medicine, Kita-ku, Kita 14, Nishi 5, Sapporo 060-8648, Japan
e-mail: t-kamiya@med.hokudai.ac.jp

Y. Asahi
e-mail: yoh-hibana@yk2.so-net.ne.jp

Y. Matsuno
Department of Pathology, Hokkaido University Hospital, Sapporo, Hokkaido, Japan

S. Todo
Department of Transplantation Surgery, Hokkaido University Hospital, Sapporo, Hokkaido, Japan

Introduction

Chondromas are the most common of all bone tumors, accounting for 35 % of benign bone tumors, 65 % of which develop around the knee or proximal humerus [1]. Malignant transformation to chondrosarcoma can occur and the presence of multiple chondromas is associated with a higher risk of malignant transformation than a solitary chondroma [2, 3]. Extraskeletal or soft tissue chondroma is a relatively rare tumor that occurs in extraosseous and extrasynovial locations [4]. More than 80 % of extraskeletal chondromas develop in the fingers or feet [5], but other unusual locations reported include the tongue [6], parotid gland [7], and liver [8]. Chondroma of the diaphragm is also very rare, with only a few cases reported [9, 10]. We report a case of chondroma of the diaphragm, which was diagnosed initially as a liver tumor with calcification, based on pre and intraoperative examinations.

Case report

A 31-year-old woman was referred to our department from another hospital, for investigation and treatment of suspected alveolar echinococcosis. She had become conscious of a slowly progressing tumor in her right upper abdomen about 4 years before consulting the first hospital and had recently been suffering from abdominal pain and anorexia. She reported having lost 3 kg in weight when she first presented. Computed tomography (CT) performed at the previous hospital showed a tumor with calcification in the right lobe of the liver. She had no relevant personal or family medical history, no history of blood transfusion, and no history of drinking swamp water. She had lived in

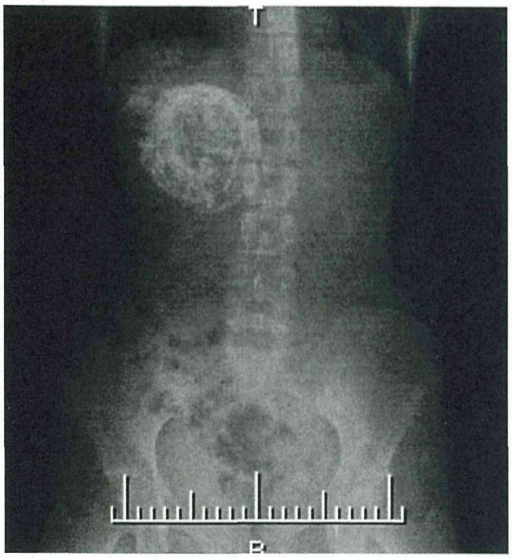

Fig. 1 Abdominal X-ray, showing a 13 × 10 cm tumor with calcification in the right upper region

Hokkaido, in the northern part of Japan, since she was born.

On examination, her abdomen was soft, but a hard fist-sized tumor was detected in the right upper quadrant. There were no signs of vascular spider, erythema palmare, abdominal varicose veins, or pedal edema. Laboratory examinations showed no signs of Hepatitis B or Hepatitis C virus infection, and serum levels of the tumor markers AFP, CEA, and CA19-9 were within the normal ranges. Serological tests by both Western blotting and enzyme-linked immunosorbent assays (ELISA) [11] were negative for echinococcosis. Abdominal X-ray showed a 13 × 10 cm tumor with calcification in the right upper region (Fig. 1). A dynamic CT study of her liver showed a 10.7 × 9.8 cm tumor in the right anterior and left medial section of the liver. The tumor was clear but had irregular boundaries and a calcified layer, and inside, it appeared as an area of low density. The tumor was not enhanced by contrast agent in any phase (Fig. 2a). There was also a thin low-density area around the calcification, and some parts of the border between this low-density area and the diaphragm were obscure (Fig. 2b). The right branch of the portal vein had narrowed as a result of compression by the tumor, but the border between the portal vein and the tumor was distinct. The middle hepatic vein was not depicted. T1-weighted magnetic resonance images (MRI) showed an area of low signal intensity within the tumor, while T2-weighted MRI showed an area of high signal intensity in the corresponding region. The region around this area had no evidence of a calcified layer, which agreed with the CT findings (Fig. 3a). Fluorodeoxyglucose positron emission tomography (FDG-PET) showed no FDG accumulation in the tumor. There was little evidence to suggest that the tumor was malignant; however, we could not rule it out.

As the patient was in pain and the tumor was progressing, we performed laparotomy, which revealed a calcified tumor in the right anterior section and atrophy of

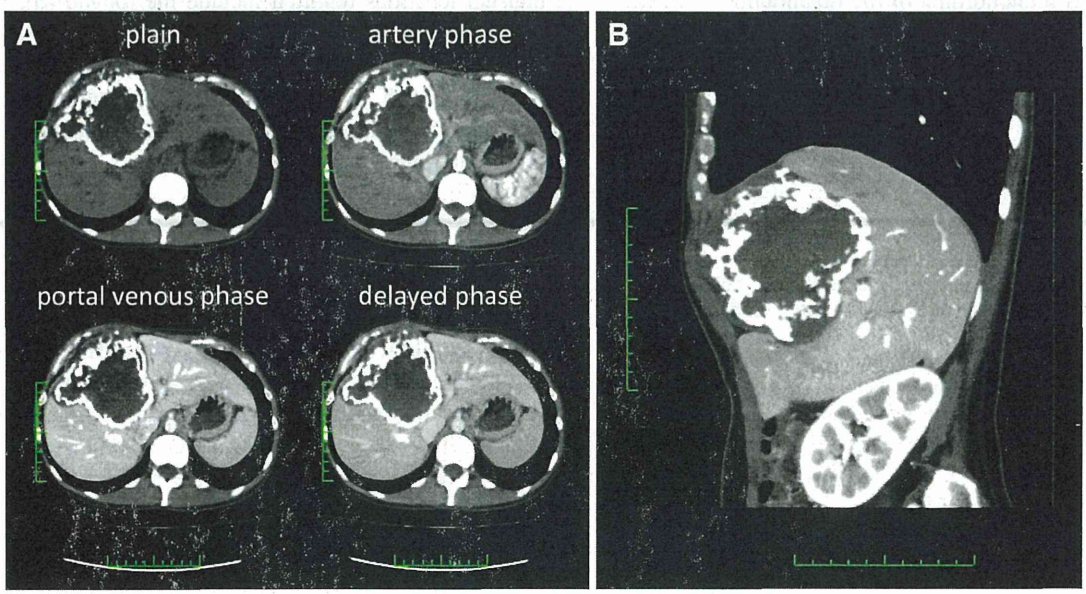

Fig. 2 a Dynamic computed tomographic (CT) images of the liver, showing a 10.7 × 9.8 cm tumor in the right anterior and left medial sections. The tumor was covered with a calcified layer, but was not enhanced by contrast agent in any phase, suggesting that there was no blood supply to it. **b** Sagittal section of the tumor on enhanced CT. Some parts of the border between the tumor and right diaphragm were obscure

the left medial section of the liver, which was being compressed by the tumor. There was continuity between the tumor and the liver, as well as between the tumor and some parts of the diaphragm (Fig. 4a). These findings were strongly suggestive that the tumor had originated from the liver. We resected the tumor with some margin, resulting in partial resection of right anterior segment and left medial segmentectomy of the liver, with partial resection of the diaphragm. The liver resection was performed by Pringle's maneuver occlusion using an ultrasonically activated scalpel in combination with a radiofrequency dissecting sealer [12]. Macroscopically, the extirpated tumor was covered by a hard calcified layer, 2–4 cm thick, and contained a cavity with necrotic tissue inside (Fig. 4b).

Pathological examination of the tumor revealed that it consisted of cartilage cells surrounded by cartilage matrices. There was no significant cellular atypia and the number of mitotic figures was within the normal range (Fig. 5a). The tumor was clearly separated from the liver by a fibrous capsule (Fig. 5b). No fibrous capsule was seen between the tumor and the diaphragm (Fig. 5c), suggesting that the tumor was contiguous with the diaphragm. Therefore, the tumor was diagnosed as a chondroma of the diaphragm. The patient had an uneventful postoperative course and her abdominal symptoms improved after the operation. There was no evidence of recurrence at her 3-year follow-up.

Discussion

Chondroma of the diaphragm has rarely been reported [9]. Initially, the tumor in the present case was considered to be a liver tumor with calcification, based on the preoperative examinations. The differential diagnoses of liver tumors with calcification include malignant tumors, infection, and

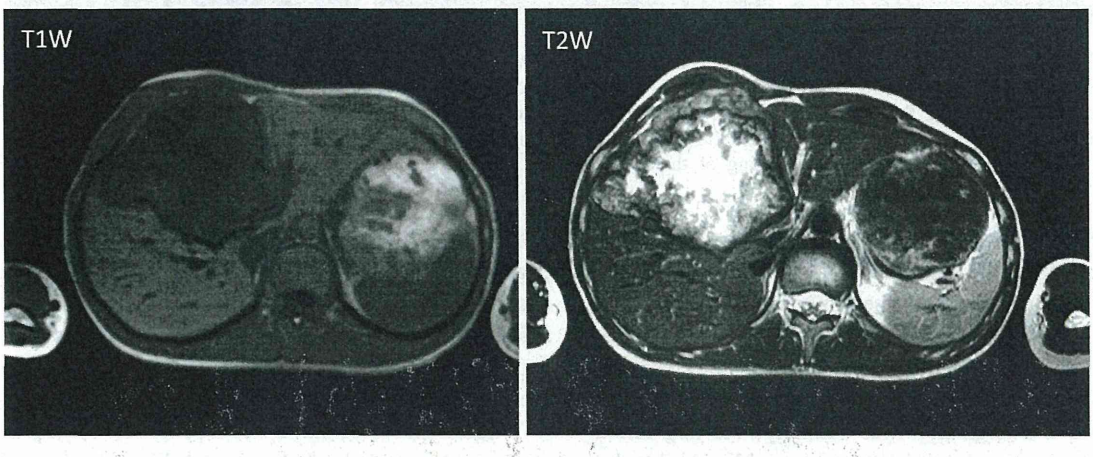

Fig. 3 Magnetic resonance imaging (MRI) showed an area of low signal intensity within the tumor on T1-weighted images and an area of high signal intensity in the corresponding region on T2-weighted images. The region around this area did not display any signals

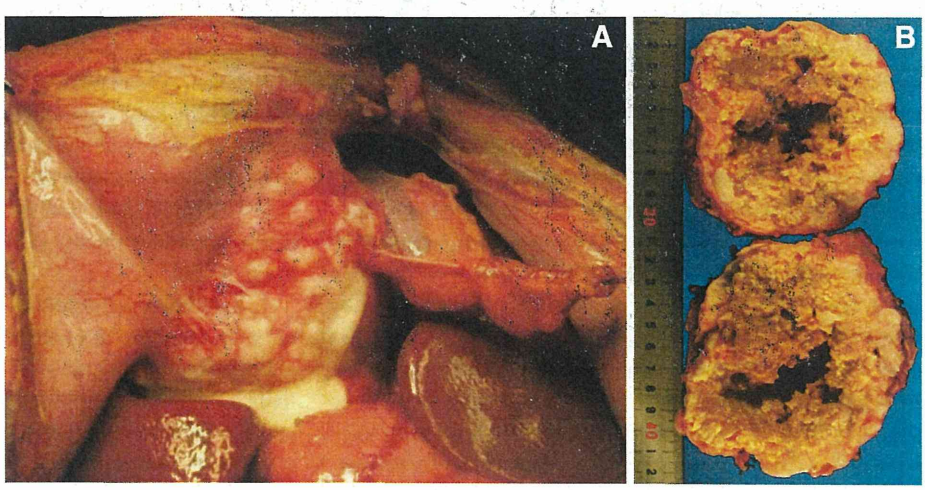

Fig. 4 **a** Intraoperative findings. The tumor was located mainly in the right lobe of the liver and had some continuity with the liver parenchyma. The tumor was also contiguous with the diaphragm. **b** Macroscopic findings of a cross-section of the tumor. The tumor was covered with a calcified layer, with some necrotic tissue inside it

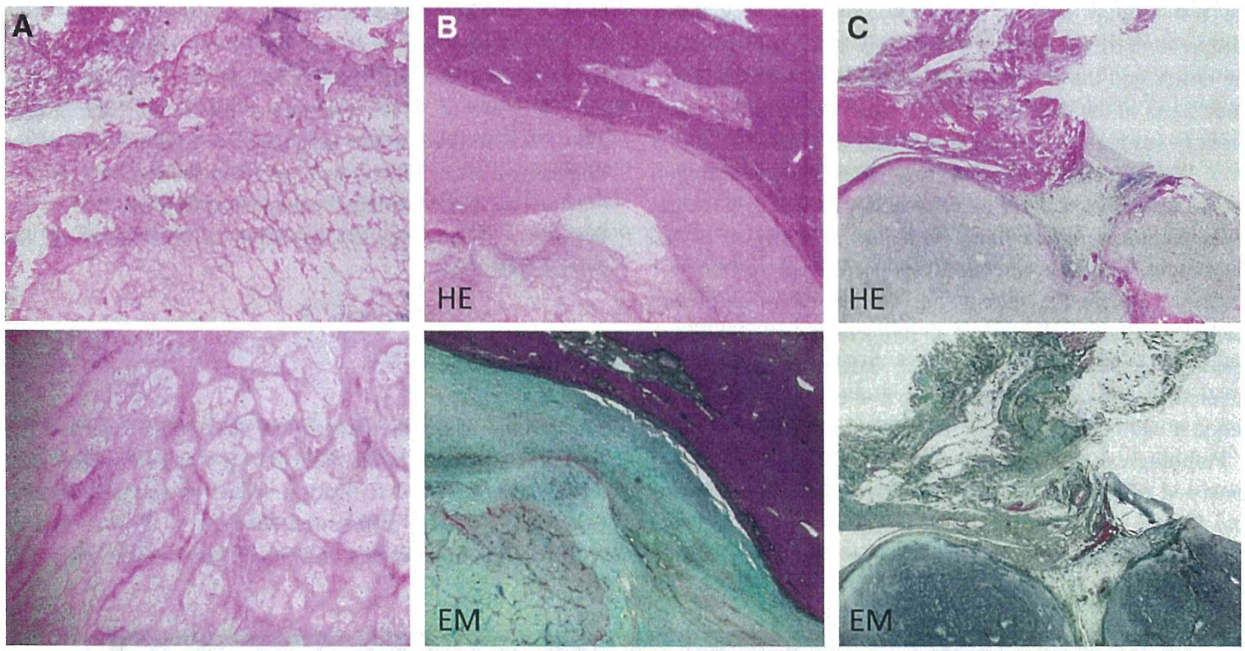

Fig. 5 **a** HE staining of the tumor showed that it consisted of cartilage cells surrounded by cartilage matrices. There was no significant cellular atypia and the number of mitotic figures was within the normal range. Original magnification ×100 (*upper*), ×400 (*bottom*). **b** HE and Elastica-Masson (EM) staining of the border between the tumor and the liver. The tumor was clearly separated from the liver by a fibrous capsule. **c** HE and EM staining of the border between the tumor and the diaphragm. No fibrous capsule was seen between the tumor and the diaphragm

benign tumors [13]. Our patient was young, without any background of hepatic disease, including hepatitis B or C. Moreover, the progression of the tumor was very slow and tests for tumor markers were negative. Preoperative imaging, including dynamic CT and MRI studies, showed no signs of a malignant tumor [14]; therefore, it was considered that a malignancy was unlikely. At her initial presentation to our department, we considered alveolar echinococcosis because of where she lived [15], but this was ruled out by a blood examination. Therefore, a benign liver tumor with calcification was suspected, as malignancy or infection was unlikely.

Distinguishing diaphragmatic tumors from abdominal tumors can be difficult, since no single imaging modality can differentiate them, especially when the tumor is located in the right diaphragm [16]. In a previous case report of chondroma of the diaphragm, the clinicians had found it difficult to establish whether the tumor had arisen in the liver or diaphragm, based on preoperative imaging and it was confirmed to be a diaphragmatic tumor only during laparoscopy [9]. Similarly, in the present case, both preoperative and intraoperative examinations suggested a liver tumor with calcification. Although intraoperative examination revealed that the tumor was contiguous with the diaphragm, it was also found to be contiguous with the liver parenchyma. Moreover, the main part of the tumor was located in the right lobe of the liver. Pathological examination subsequently confirmed that the tumor was a chondroma. The primary location of the tumor was considered to be the diaphragm because there was continuity between the tumor and diaphragm and the border between the tumor and liver was distinct.

Three hypotheses have been proposed to explain the etiology of extraskeletal chondroma. First, the migration of cartilage cells originating from the adjacent skeletal structure to connective tissues; second, conversion of the precartilaginous tissues in the ligament attachment area to an activation period; and third, metaplasia of synovial cells, differentiating to cartilage [17].

Surgical resection of a wide local area is recommended for extraskeletal chondroma, considering the 10–15 % recurrence rate and the fact that it relieves the symptoms caused by compression of the surrounding organs [18–20]. Our patient had abdominal symptoms, consistent with diaphragmatic tumors [16], which improved after the operation.

In summary, we report this case to show that chondroma of the diaphragm, despite its rarity, should be considered in the differential diagnosis of a calcified tumor located in the liver, which has continuity with the diaphragm. Pathological examination of the tumor, liver, and diaphragm can allow us to diagnose the tumor origin.

Conflict of interest Yoh Asahi and his co-authors have no conflicts of interest.

References

1. Lee KC, Davies AM, Cassar-Pullicino VN. Imaging the complications of osteochondromas. Clin Radiol. 2002;57:18–28.
2. Altay M, Bayrakci K, Yildiz Y, Erekul S, Saglik Y. Secondary chondrosarcoma in cartilage bone tumors: report of 32 patients. J Orthop Sci. 2007;12:415–23.
3. Woertler K. Benign bone tumors and tumor-like lesions: value of cross-sectional imaging. Eur Radiol. 2003;13:1820–35.
4. Falleti J, De Cecio R, Mentone A, Lamberti V, Friscia M, De Biasi S, et al. Extraskeletal chondroma of the masseter muscle: a case report with review of the literature. Int J Oral Maxillofac Surg. 2009;38:895–9.
5. Papagelopoulos PJ, Savvidou OD, Mavrogenis AF, Chloros GD, Papaparaskeva KT, Soucacos PN. Extraskeletal chondroma of the foot. Jt Bone Spine. 2007;74:285–8.
6. Sera H, Shimoda T, Ozeki S, Honda T. A case of chondroma of the tongue. Int J Oral Maxillofac Surg. 2005;34:99–100.
7. Aslam MB, Haqqani MT. Extraskeletal chondroma of parotid gland. Histopathology. 2006;48:465–7.
8. Fried RH, Wardzala A, Willson RA, Sinanan MN, Marchioro TL, Haggitt R. Benign cartilaginous tumor (chondroma) of the liver. Gastroenterology. 1992;103:678–80.
9. Itakura M, Shiraishi K, Kadosaka T, Matsuzaki S. Chondroma of the diaphragm—report of a case. Endoscopy. 1990;22:276–8.
10. Clagett OT, Johnson MA 3rd. Tumors of the diaphragm. Am J Surg. 1949;78:526–30.
11. Furuya K, Sato N, Uchino J. Enzyme-linked immunosorbent assay (ELISA) and western blotting (WB) test. Hokkaido Univ Med Libr Ser. 1993;83:75–91.
12. Yokoo H, Kamiyama T, Nakanishi K, Thara M, Fukumori D, Kamachi H, Matsushita M, Todo S. Effectiveness of using ultrasonically activated scalpel in combination with radiofrequency dissecting sealer or irrigation bipolar for hepatic resection. Hepatogastroenterology. 2012;59:831–5.
13. Stoupis C, Taylor HM, Paley MR, Buetow PC, Marre S, Baer HU. The Rocky liver: radiologic-pathologic correlation of calcified hepatic masses. Radiographics. 1998;18:675–85.
14. Haruki K, Wakiyama S, Shiba H, Ishida Y, Yanaga K. Intrahepatic arterioportal shunt mimicking a metastatic liver tumor: report of a case. Surg Today. 2012;42:391–4.
15. Yoshida T, Kamiyama T, Okada T, Nakanishi K, Yokoo H, Kamachi H. Alveolar echinococcosis of the liver in children. J Hepatobiliary Pancreat Sci. 2010;17:152–7.
16. Zhang Y, Zhang SC, Ren WD, Wang WL, Zhou X. Primary yolk sac tumor in diaphragm. Pediatr Surg Int. 2012;28:1157–60.
17. Kwon H, Kim HY, Jung SN, Sohn WI, Yoo G. Extraskeletal chondroma in the auricle. J Craniofac Surg. 2010;21:1990–1.
18. Watanabe F, Saiki T, Ochochi Y. Extraskeletal chondroma of the preauricular region: a case report and literature review. Case Rep Med. 2012;2012:121743.
19. Cumming D, Massraf A, Jones JW. Extraskeletal chondroma as a cause of carpal tunnel syndrome: a case report. Hand Surg. 2005;10:327–30.
20. Singh AP, Dhammi IK, Jain AK, Bhatt S. Extraskeletal juxtaarticular chondroma of the knee. Acta Orthop Traumatol Turc. 2011;45:130–4.

Surg Today (2014) 44:2339–2344
DOI 10.1007/s00595-014-0935-z

ORIGINAL ARTICLE

The differences in microorganism growth on various dressings used to cover injection sites: inspection of the risk of catheter-related bloodstream infections caused by Gram-negative bacilli

Hideki Kawamura · Norihiko Takahashi · Masahiro Takahashi · Akinobu Taketomi

Received: 25 November 2013 / Accepted: 7 April 2014 / Published online: 29 May 2014

Abstract
Purposes Sepsis caused by Gram-negative bacilli (GNB) is the most serious catheter-related bloodstream infection. However, the cause(s) of GNB propagation on the skin around needle or catheter insertion sites remain unclear. This observational study aimed to assess the differences in the microbial growth among various types of dressings used to cover injection sites, with a particular focus on GNB.
Methods We analyzed the bacterial populations on three types of surgical dressings; Tegaderm I.V. (semi-permeable, 27 sheets), IV3000 (highly permeable, 34 sheets) and Tegaderm CHG (chlorhexidine-impregnated, 26 sheets). The peripheral catheter site dressing was replaced every 3 days or when there was leakage or pain at the catheter site.
Results Bacterial growth was observed in all Tegaderm I.V. and IV3000 sheets and in only one (3.8 %) Tegaderm CHG sheet. The GNB detection rate was significantly lower in the IV3000 group (2.9 %) than in the Tegaderm I.V. group (63.0 %). No GNB growth was identified in the Tegaderm CHG group.
Conclusions Semi-permeable dressings were insufficient to prevent GNB infections, whereas highly permeable or chlorhexidine-impregnated dressings could prevent GNB infections. Chlorhexidine-impregnated dressings can control almost all bacterial growth.

H. Kawamura (✉) · M. Takahashi
Department of Surgery, JA Sapporo Kosei Hospital, N3, E8, Chuo-ku, Sapporo 060-0033, Japan
e-mail: h.kawamura@med.hokudai.ac.jp

N. Takahashi · A. Taketomi
Department of Gastroenterological Surgery I, Hokkaido University Graduate School of Medicine, Sapporo, Japan

Keywords Gram-negative bacillus · Catheter-related bloodstream infection · Dressing · Sepsis

Introduction

The management of many diseases requires intravenous infusions. In particular, in patients who undergo gastrointestinal surgery, the return to oral intake is prolonged and the quantitative intake is therefore insufficient, thus resulting in longer periods of intravenous alimentation compared with other surgeries. Therefore, such surgeries portend a higher risk of catheter-related bloodstream infection (CRBSI). Although catheter management guidelines focused on CRBSI prevention have already been created and are currently implemented in most facilities, CRBSI continues to be prevalent [1–3]. Sepsis caused by Gram-negative bacilli (GNB) is the most serious CRBSI. The mortality rate from endotoxin shock is approximately 50 % in such cases, despite appropriate antimicrobial therapy and optimum supportive care [4]. Both the skin at the needle or catheter insertion site (extraluminal source) and the catheter connector/hub (intraluminal source) are considered to be sources of CRBSI; however, most of the recent CRBSIs occurred extraluminally in patients for whom CRBSI prevention guidelines were applied [5, 6]. Therefore, a close relationship appears to exist between bacterial colonization of the skin and the bacterial species responsible for CRBSI. The identification of skin conditions that promote GNB propagation is important to help prevent CRBSI caused by GNB. However, although there have been several reports on the rate of CRBSI and GNB, none have assessed the differences in the microbiology associated with various skin conditions [7–9]. Therefore, this observational study aimed to assess the skin

microbiology using various dressings among surgical patients, with a particular focus on GNB.

We cultured representative samples of three different types of transparent dressings in this study. Currently, most guidelines for the prevention of CRBSI recommend that the injection site should be covered with a sterile, transparent, semi-permeable dressing if the patient is not diaphoretic or if the site is not bleeding or oozing [1]. Naturally, the bacterial flora in the skin under such dressings is predicted to be different from that in exposed skin. Therefore, an evaluation of the microorganisms on and in the skin under dressings is very important to elucidate the source of extraluminal bacteria causing CRBSI.

Materials and methods

We evaluated the influence of three types of transparent surgical dressings on the bacterial populations of the skin; the Tegaderm I.V. (3M Health Care, St. Paul, MN, USA), a semi-permeable dressing; IV3000 (Smith & Nephew plc., London, UK), a highly permeable dressing and Tegaderm CHG (3M Health Care), a chlorhexidine-impregnated dressing. The peripheral catheter site dressing was replaced every 3 days or when there was leakage or pain at the catheter site. Surgical patients with gastric or colorectal cancer, which accounted for the majority of surgical cases treated at our institute, were assessed. The study of the Tegaderm I.V. dressing cultures was performed using 27 dressing sheets obtained as samples from 11 patients with gastric cancer and six patients with colorectal cancer between August 2012 and October 2012. Surgical staff wearing new, unsterilized medical gloves peeled the dressings with their hands and placed them in a sterilized laboratory dish for culture. For the IV3000 dressing culture, 34 sheets were collected from 10 patients with gastric cancer and eight patients with colorectal cancer between October 2012 and November 2012. Each dressing was peeled and cultured as described above. For the Tegaderm CHG dressing culture, 26 sheets were obtained from 11 patients with gastric cancer and seven patients with colorectal cancer between January 2013 and February 2013. Each dressing was peeled as described above and cultured after removing the unattached chlorhexidine-impregnated gel.

To evaluate the influence of the bacteria present on the exposed skin of surgical patients, skin flora samples were collected on the scheduled showering day from 45 consecutive patients undergoing gastrectomy. These patients underwent surgery between August 2011 and December 2012. The afternoon on preoperative day 1 was recorded as the last instance of preoperative showering, and the afternoon on postoperative day 6 was recorded as the first instance of postoperative showering in these patients. Bacterial samples were collected on the mornings of preoperative day 1 and postoperative day 6 by rubbing the skin surface with aseptic cotton swabs designed for bacterial culture at regions of open skin on the forearm and clavicle, which were often used as injection sites.

Many recent comparative studies have been performed administered under institutional review board (IRB) approval; however, this study had not been submitted to the IRB, because it did not include treatments, any impact on the diseases, or any effect that might have increased the patient's physical suffering or costs. To obtain informed consent, we verbally explained the purpose of this study to all patients, all of whom agreed to participate in the study. The cost of dressings and bacterial cultures were borne by the hospital under approval.

Statistical analysis

The statistical analyses were performed using the t test, Pearson's Chi-square test and Tukey's honestly significant difference (HSD) test. The SPSS 16.0 for Windows software program (SPSS Inc., Chicago, IL, USA) was used for all of the statistical analyses. A probability (p) value <0.05 was considered to be statistically significant.

Results

Patient demographics

There were no significant differences in the patient age, sex or surgery type among the Tegaderm I.V., IV3000 and Tegaderm CHG groups (Table 1). Only peripheral catheter site dressings were used in all groups. There was also no significant difference among the groups in the mean duration of dressing application (Table 1).

Detection of bacterial growth detection in dressing cultures

Bacterial growth was detected in all dressing sheets obtained from the Tegaderm I.V. (27/27 100 %) and IV3000 (34/34 100 %) groups, but in only one (1/26 3.8 %) sheet obtained from the Tegaderm CHG group (Table 2). The bacteria detected in all groups are summarized in Table 3. Notably, the GNB detection rate was significantly lower in the IV3000 group (1/34 2.9 %) than in the Tegaderm I.V. group (17/27 63.0 %; Table 4), whereas no GNB growth was detected in the Tegaderm CHG group (0/26). No CRBSI developed in this series.

Table 1 The background of the patients in terms of the dressing culture, catheter type and duration of attachment

	Tegaderm I.V. ($n = 17$)	IV3000 ($n = 18$)	Tegaderm CHG ($n = 18$)	p
Age	71.7 ± 12.9	66.9 ± 11.1	68.3 ± 11.0	0.235
Gender				0.551
Male	12 (70.6 %)	11 (61.1 %)	14 (77.8 %)	
Female	5 (29.4 %)	7 (38.9 %)	4 (22.2 %)	
Operation				0.246
Gastrectomy	11 (64.7 %)	8 (44.4 %)	11 (61.1 %)	
Colorectal surgery	6 (35.3 %)	10 (55.6 %)	7 (38.9 %)	

	Tegaderm I.V. ($n = 27$)	IV3000 ($n = 34$)	Tegaderm CHG ($n = 26$)	p
Mean duration of attachment (days)	4.2 ± 1.6	2.9 ± 1.7	3.0 ± 1.9	0.061*

CV central venous

*Tegaderm I.V. versus IV3000

Detection of bacteria in exposed skin cultures

In this study, skin bacterial samples were collected from 29 males and 16 females, with a mean age of 68.4 ± 10.6 (range 33–86) years. No significant difference was observed in the detection rate of bacteria in cultures from the forearm (44.4 vs. 31.1 %) and clavicle (62.2 vs. 42.2 %) on preoperative day 1 and postoperative day 6. Furthermore, no GNB were detected in any of the samples (Table 5). The results of the microbiological analyses of the skin cultures are presented in Table 6.

Table 2 The detection of bacteria in the dressing cultures

	Tegaderm I.V. ($n = 27$)	IV3000 ($n = 34$)	Tegaderm CHG ($n = 26$)	p
Detection				0.000
Yes	27 (100 %)	34 (100 %)	1 (3.8 %)	
No	0 (0 %)	0 (0 %)	25 (96.2 %)	

Discussion

The incidence of CRBSI in surgical patients has previously been reported to be 0.49–0.9 %, with a mortality rate of 15–19.6 % in these cases [10–12]. In our department, the incidence rate of CRBSI in surgical patients was 0.6 % (40/6620) from 2004 to 2010, which was virtually the same as that in previous reports [10–12]. GNB are considered to be

Table 3 The microbiological findings of the dressing culture

Tegaderm I.V. ($n = 27$)	Cases	IV3000 ($n = 34$)	Cases	Tegaderm CHG ($n = 26$)	Cases
Bacillus species	21	*Bacillus* species	32	*Bacillus* species	1
Staphylococcus epidermidis	13	*Staphylococcus epidermidis*	3		
Enterococcus faecalis	9	*Staphylococcus aureus*	3		
Staphylococcus aureus	3	*Enterococcus faecalis*	2		
Staphylococcus haemolyticus	1	*Corynebacterium species*	1		
Corynebacterium species	1	*Enterococcus agglomerans*	1		
Enterococcus gallinarum	1	*Enterococcus faecium*	1		
Staphylococcus capitis subspecies *ureoly*	1	*Staphylococcus haemolyticus*	1		
Streptococcus mitis group	1	*Staphylococcus hominis*	1		
Acinetobacter baumannii/haemolyticus[a]	6	*Staphylococcus intermedius*	1		
Enterobacter cloacae[a]	3	*Staphylococcus lugdunensis*	1		
Acinetobacter iwoffi[a]	3	*Staphylococcus warneri*	1		
Enterobacter gergoviae[a]	2	*Pseudomonas fluorescens/putida*[a]	1		
Pseudomonas aeruginosa[a]	1				
Stenotrophomonas maltophilia[a]	1				

[a] Gram-negative bacillus

Table 4 The differences in the bacteria between the Tegaderm I.V. and IV3000

	Tegaderm I.V. ($n = 27$)	IV3000 ($n = 34$)	p
Microbiology			0.000
Non-GNB	10 (37.0 %)	33 (97.1 %)	
GNB	17 (63.0 %)	1 (2.9 %)	

GNB Gram-negative bacillus

Table 5 The detection of bacteria in skin cultures, and the types of bacteria detected

	Preoperative day 1	Postoperative day 6	p
Forearm ($n = 45$)			
Bacteria detection			0.277
Yes	20 (44.4 %)	14 (31.1 %)	
No	25 (55.5 %)	31 (68.9 %)	
Microbiology			
GNB	0 (0 %)	0 (0 %)	
Non-GNB	20 (100 %)	14 (100 %)	
Neck ($n = 45$)			
Bacteria detected			0.091
Yes	28 (62.2 %)	19 (42.2 %)	
No	17 (37.8 %)	26 (57.8 %)	
Microbiology			
GNB	0 (0 %)	0 (0 %)	
Non-GNB	28 (100 %)	19 (100 %)	

GNB Gram-negative bacillus

important pathogens in all CRBSIs. The incidence of CRBSI caused by GNB is reportedly 16.0–39.6 %, and the mortality rate for endotoxic shock is approximately 50 % [4, 7, 8]. The primary causes of CRBSI include contamination during preparation of infusion bottles, inadequate aseptic techniques during catheter insertion and manipulation of the catheter hub and connection ports. Therefore, guidelines for CRBSI prevention describe preventive measures [13–15]. These guidelines recommend the use of aseptic techniques during catheter insertion and cutaneous aseptic preparation as measures to prevent extraluminal bacterial infiltration; furthermore, for the management of bacterial proliferation after insertion, they recommend periodic dressing changes or reinsertion for routine use [2, 3, 13–15]. However, CRBSI continue to be prevalent, and no guidelines currently describe independent measures for the prevention of CRBSI caused by GNB that are not part of the normal bacterial flora in the skin.

In typical cases, the guidelines recommend that injection sites should be covered with sterile, transparent, semi-permeable dressings [1, 16]. The condition of the skin under a dressing is obviously different from that of exposed skin. Therefore, understanding the bacterial growth conditions of the skin under dressings is important to prevent CRBSI. However, to our knowledge, no previously published report has addressed this issue. In the present study, Tegaderm I.V. was selected as a semi-permeable dressing. These dressings are designed such that they are better than impermeable transparent dressings, which allow moisture accumulation around the insertion site and potentiate bacterial growth. However, all Tegaderm I.V. dressing cultures demonstrated bacterial growth, and 57.1 % included GNB. This result indicates that semi-permeable dressings are insufficient for preventing CRBSI caused by not only normal bacterial flora, but also GNB, even if the guidelines were followed.

IV3000 is a highly permeable transparent dressing, and its moisture vapor transmission rate has been reported to be exceptionally high (11,140 g/m^2/24 h) compared with that of semi-permeable film dressings (400–900 g/m^2/24 h) [17]. The advantages of this product include less dressing

Table 6 The microbiological findings of the skin cultures

Preoperative day 1	Cases	Postoperative day 6	Cases
Forearm ($n = 45$)			
Staphylococcus hominis	7	*Staphylococcus epidermidis*	6
Bacillus species	6	*Staphylococcus hominis*	3
Staphylococcus epidermidis	6	*Bacillus* species	2
Staphylococcus haemolyticus	3	*Staphylococcus capitis*	2
		Staphylococcus haemolyticus	1
		Staphylococcus saprophyticus	1
		Streptococcus sanguis	1
Neck ($n = 45$)			
Staphylococcus hominis	10	*Bacillus* species	9
Bacillus species	8	*Staphylococcus epidermidis*	7
Staphylococcus epidermidis	6	*Staphylococcus hominis*	4
Staphylococcus haemolyticus	2	*Micrococcus* species	1
Staphylococcus species	1	*Staphylococcus capitis* subspecies	1
Staphylococcus capitis	1	*Staphylococcus schleiferi*	1
Staphylococcus haemolyticus	1	*Streptococcus sanguis*	1
Staphylococcus species	1		

lift-up and longer intervals between dressing changes; however, these factors have been shown to have no influence on the incidence of CRBSI [9, 18]. The findings of the present study also do not suggest a decreased risk of CRBSI with IV3000 dressings, because bacterial growth was observed in all IV3000 cultures. However, GNB growth was observed in only 1 (2.9 %) IV3000 sheet. No previous study has reported the bacterial type in CRBSI associated with the use of highly permeable transparent dressings, and our present results suggest that the IV3000 dressings could decrease the incidence of CRBSI caused by GNB, and thus may be superior to Tegaderm I.V..

Tegaderm CHG is a chlorhexidine-impregnated dressing used to suppress bacterial growth at injection sites and decrease the incidence of CRBSIs [6, 12]. In this study, bacterial growth was observed in only one (3.8 %) Tegaderm CHG sheet, and theses bacteria were not GNB. This dressing may inhibit CRBSI caused by not only GNB, but also several other types of skin bacteria. However, there are some notable limitations associated with the routine use of this product. First, the Tegaderm CHG dressing is extremely expensive; a 7 × 8.5-cm sheet costs 1,100 yen. On the other hand, a 7 × 9-cm IV3000 sheet costs 150 yen. Therefore, the cost/benefit of Tegaderm CHG dressings should be taken into account. Furthermore, the potential existence or development of resistance to chlorhexidine is an important factor. There have already been some reports on chlorhexidine-resistant bacterial infections [19, 20]. Therefore, the recent guidelines suggest the restrictive use of chlorhexidine-impregnated dressings; if the CRBSI rate does not decrease despite adherence to basic preventive measures, including education and training, chlorhexidine can be used for skin antisepsis [16].

There was one factor that could have influenced the results in this dressing culture study. The dressing cultures reflected both sides of the dressing faces (skin side and opposite side). To solve this problem, the examination of the skin bacterial condition under an exposed environment would probably be useful. In this study, no significant difference was observed in the detection rate of skin bacterial cultures between preoperative day 1 and postoperative day 6; furthermore, no GNB appeared on the exposed skin either pre- or postoperatively. Therefore, we believe that the overall condition of bacterial growth under the dressings was accurately reflected by our results. Moreover, our results suggest that GNB, the primary target of this study, did not propagate under open conditions, and thus, the GNB detected in the cultures of the dressings were not due to exterior (non-skin-side) bacteria.

In conclusion, semi-permeable dressings are insufficient for preventing GNB infections, whereas highly permeable and chlorhexidine-impregnated dressings may be effective for controlling CRBSI caused by GNB. Furthermore, chlorhexidine-impregnated dressings can control almost all bacterial growth and may be the most effective dressing to prevent CRBSI, although their cost and the potential for the development of bacterial resistance must also be taken into consideration. A large randomized study focusing on the correlation between the dressing type and GNB CRBSI rate will be needed to confirm the present findings.

Conflict of interest Drs. Hideki Kawamura, Norihiko Takahashi, Masahiro Takahashi and Akinobu Taketomi have no conflicts of interest or financial interests to disclose.

References

1. O'Grady NP, Alexander M, Dellinger EP, Gerberding JL, Heard SO, Maki DG, et al. Guidelines for the prevention of intravascular catheter-related infections. Centers for Disease Control and Prevention. MMWR Recomm Rep. 2002;9:1–29.
2. Crosby CT, Tsj E, Lambert PA, Adams D. Preoperative skin preparation: a historical perspective. Br J Hosp Med. 2009;70:579–82.
3. Popovich KJ, Hota B, Hayes R, Weinstein RA, Hayden MK. Effectiveness of routine patient cleansing with chlorhexidine gluconate for infection prevention in the medical intensive care unit. Infect Control Hosp Epidemiol. 2009;30:959–63.
4. Periti P. Current treatment of sepsis and endotoxaemia. Expert Opin Pharmacother. 2000;1:1203–17.
5. Mermel LA. What is the predominant source of intravascular catheter infections? Clin Infect Dis. 2011;52:211–2.
6. Timsit JF, Mimoz O, Mourvillier B, Souweine B, Garrouste-Orgeas M, Alfandari S, et al. Randomized controlled trial of chlorhexidine dressing and highly adhesive dressing for preventing catheter-related infections in critically ill adults. Am J Respir Crit Care Med. 2012;186:1272–8.
7. Velasco E, Soares M, Byington R, Martins CA, Schirmer M, Dias LM, et al. Prospective evaluation of the epidemiology, microbiology, and outcome of bloodstream infections in adult surgical cancer patients. Eur J Clin Microbiol Infect Dis. 2004;23:596–602.
8. Pujol M, Hornero A, Saballs M, Argerich MJ, Verdaguer R, Cisnal M, et al. Clinical epidemiology and outcomes of peripheral venous catheter-related bloodstream infections at a university-affiliated hospital. J Hosp Infect. 2007;67:22–9.
9. Reynolds MG, Tebbs SE, Elliott TS. Do dressings with increased permeability reduce the incidence of central venous catheter related sepsis? Intensive Crit Care Nurs. 1997;13:26–9.
10. Humphreys H, Newcombe RG, Enstone J, Smyth ET, McIlvenny G, Fitzpatrick F, et al. Four country healthcare associated infection prevalence survey 2006: risk factor analysis. J Hosp Infect. 2008;69:249–57.
11. Zingg W, Pittet D. Peripheral venous catheter: an under-evaluated problem. Int J Antimicrob Agents. 2009;34:38–42.
12. Timsit JF, Schwebel C, Bouadma L, Geffroy A, Garrouste-Orgeas M, Pease S, et al. Chlorhexidine-impregnated sponges and less frequent dressing changes for prevention of catheter-related infections in critically ill adults: a randomized controlled trial. JAMA. 2009;301:1231–41.
13. Koerner RJ, Morgan S, Ford M, Orr KE, McComb JM, Gould FK. Outbreak of gram-negative septicaemia caused by contaminated continuous infusions prepared in a non-clinical area. J Hosp Infect. 1997;36:285–9.
14. Ball C. Hospital-acquired bacteraemia—surveillance and guidelines for practice. Intensive Crit Care Nurs. 2001;17:249–53.

15. Raad II, Hanna HA. Intravascular catheter-related infections: new horizons and recent advances. Arch Intern Med. 2002;162:871–8.
16. O'Grady NP, Alexander M, Burns LA, Dellinger EP, Garland J, Heard SO, et al. Guidelines for the prevention of intravascular catheter-related infections. Am J Infect Control. 2011;39(4 Suppl 1):S1–34.
17. Jones A. Dressings for the management of catheter sites. JAVA. 2004;9:26–33.
18. Keenlyside D. Avoiding an unnecessary outcome. A comparative trial between IV3000 and a conventional film dressing to assess rates of catheter-related sepsis. Prof Nurse. 1993;8:288–91.
19. Vu-Thien H, Darbord JC, Moissenet D, Dulot C, Dufourcq JB, Marsol P, et al. Investigation of an outbreak of wound infections due to *Alcaligenes xylosoxidans* transmitted by chlorhexidine in a burns unit. Eur J Clin Microbiol Infect Dis. 1998;17:626–724.
20. Higgins CS, Murtough SM, Williamson E, Hiom SJ, Payne DJ, Russell AD, et al. Resistance to antibiotics and biocides among non-fermenting Gram-negative bacteria. Clin Microbiol Infect. 2001;7:308–15.

World J Surg (2014) 38:2716–2723
DOI 10.1007/s00268-014-2642-8

World Journal of Surgery

Comparison of Single-Incision Plus One Additional Port Laparoscopy-assisted Anterior Resection with Conventional Laparoscopy-assisted Anterior Resection for Rectal Cancer

Futoshi Kawamata · Shigenori Homma · Nozomi Minagawa · Hideki Kawamura · Norihiko Takahashi · Akinobu Taketomi

Published online: 23 May 2014

Abstract

Background Reduced-port laparoscopic surgery is the latest innovation in minimally invasive surgery. We performed single-incision plus one additional port laparoscopy-assisted anterior resection (SILS + 1-AR) starting in August 2010. This study aimed at evaluating the feasibility of SILS + 1-AR and comparing it with that of conventional laparoscopy-assisted anterior resection (C-AR).

Methods Patients with preoperative clinical stage 0 to stage III rectal cancer were included. Demographic, intraoperative, and pathological examination data, as well as short-term outcome data, of 20 patients who underwent SILS + 1-AR were retrospectively compared with that of 20 patients who underwent C-AR. Invasiveness of the two procedures was also evaluated through a vital signs diary and hematological examination on postoperative days (POD) 1, 3, and 7.

Results Operating time, mean estimated blood loss, the number of lymph nodes dissected, the number of lymph node metastases, and the mean distal resection margin length were not significantly different. However, postoperative neutrophil counts in the SILS + 1-AR group were lower than those in the C-AR group ($P = 0.085$). A significant difference in body temperature was observed in the SILS + 1-AR group on POD 1 ($P = 0.028$). No significant differences were observed in perioperative and overall morbidity between the two groups. Conversion to open surgery was required in 2 (10 %) of the 20 patients in the SILS + 1-AR group. The mean postoperative length of stay and recurrence rates were similar in the two groups.

Conclusion SILS + 1-AR for rectal cancer is similar to C-AR in safety, feasibility, and provision of oncological radicality.

F. Kawamata · S. Homma (✉) · N. Minagawa · H. Kawamura · N. Takahashi · A. Taketomi
Department of Gastroenterological Surgery I, Hokkaido University Graduate School of Medicine, North 15, West 7, Kita-ku, Sapporo 060-8638, Japan
e-mail: homma.s@nifty.com

Introduction

Laparoscopic colorectal surgery (LCS) is a safe and efficacious alternative to open colorectal surgery in the management of colorectal carcinoma [1, 2]. The short-term outcomes of the COLOR II trial showed that the radicality of laparoscopic resection (as assessed by a pathology report) in patients with rectal cancer is no different than that of open surgery, and that laparoscopic surgery was associated with similar rates of intraoperative complications, morbidity, and mortality [3]. In recent years, single-incision laparoscopic surgery (SILS) has further reduced the invasive nature of surgical procedures and provides even greater cosmetic benefits than conventional multiport laparoscopic surgery (CLS) [4]. However, the disadvantages of SILS are a loss of triangulation, interference between the instruments and the scope and the surgeon's arm and the scope, and obstruction of the operative fields due to parallel placement of the instruments [5]. These challenges are more evident in SILS for rectal procedures because of the need for adequate oncological margins and creation of a tension-free anastomosis. Current evidence for SILS provides information regarding the outcomes of right-sided colectomy for select patients by experienced surgeons [6–8]; however, the evidence for rectal cancer is limited. Adding an additional port to SILS may bridge the gap between CLS and SILS with a relatively shorter learning curve while maintaining oncological principles [9–11].

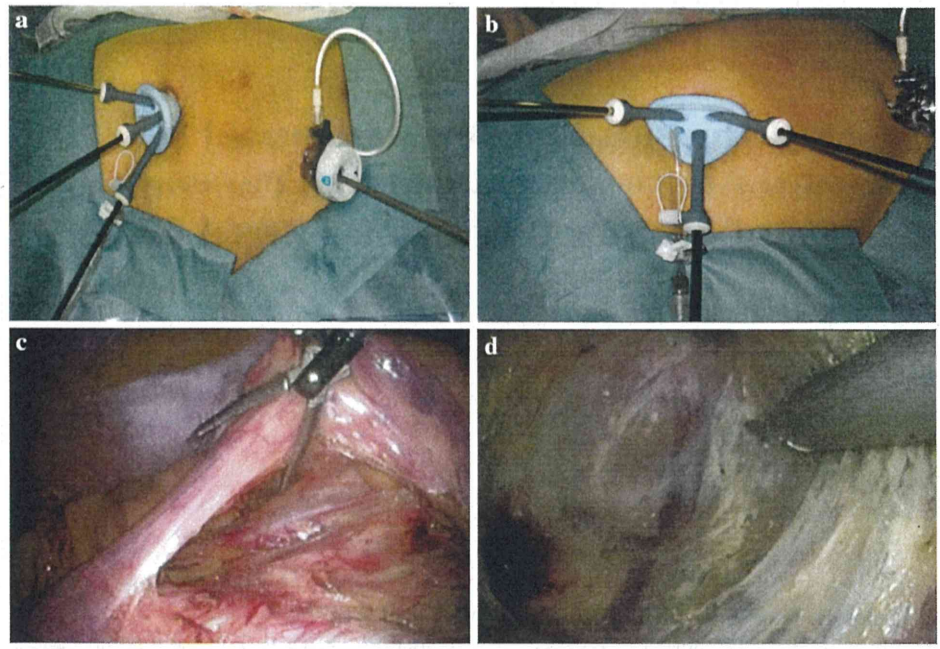

Fig. 1 **a** Port setting. In the SILS + 1-AR group, a 3-cm transumbilical incision was made and the SILS port, with three built-in trocars, was inserted into a single umbilical incision. A 12-mm port was inserted into the *right lower* quadrant of the abdomen. **b** Intraoperatively, the system allows greater freedom of movement of the instruments. **c** SILS + 1-AR with lymph node dissection around the inferior mesenteric artery. **d** All procedures had to comply with the principles of TME

We began performing single-incision plus one additional port laparoscopy-assisted anterior resection (SILS + 1-AR) in August 2010. This study aimed at evaluating the feasibility of SILS + 1-AR and comparing it with that of conventional laparoscopy-assisted anterior resection (C-AR) for rectal cancer requiring extended lymph node dissection.

Methods

Patients

We conducted a case-matched, controlled study to compare SILS + 1-AR to C-AR for rectal cancer. We included patients who had preoperative clinical stage 0 to stage III rectal cancer that required anterior resection with extended lymph node dissection. The SILS + 1-AR group included select patients who completed their treatment between August 2010 and May 2012 ($n = 20$). Patients who underwent C-AR for stage 0 to stage III rectal cancer between June 2008 and March 2012 were selected as the controls for this study ($n = 20$) and were matched to the SILS + 1-AR patients for age, sex, body mass index (BMI), history of abdominal surgery, disease type, and tumor location. We excluded T3 rectal cancers located within 2 mm of the endopelvic fascia (circumferential margin positive), determined by computed tomography (CT) or magnetic resonance imaging (MRI). Staging and tumor location were determined according to the Japanese Society for Cancer of the Colon and Rectum (JSCCR) 2010 guidelines [12]. Demographic data, intraoperative parameters, and the postoperative outcomes for the 20 patients in the SILS + 1-AR group were retrospectively compared with those of the 20 patients in the C-AR group.

Operative procedures

Three colorectal surgeons participated in this study; one surgeon performed the SILS + 1-ARs, while the other two surgeons performed the C-ARs. All patients were placed in the modified lithotomy position in Trendelenburg. In the SILS + 1-AR group, a 3-cm transumbilical incision was made and the SILS port (Covidien Ltd., Hamilton, Bermuda) with three built-in trocars was inserted into the single umbilical incision. An additional 12-mm trocar was placed in the right lower quadrant (Fig. 1a, b). A 5-mm standard-definition flexible scope was inserted in the 5-mm trocar at the extreme caudal end of the SILS port for the duration of the procedure. Activating laparoscopic coagulating shears were used for dissection. Straight and curved graspers (Roticulator Endo Grasp, Covidien Ltd.) were used to grasp the tissue. Dissection was performed using a medial-to-lateral approach while preserving the left ureter

and gonadal vessels. The dissection was continued superior to the level of the root of the inferior mesenteric artery, and high ligation of the inferior mesenteric artery was achieved (Fig. 1c). Then, the root of the superior rectal artery and inferior mesenteric vein was divided. All procedures complied with the principles of total mesorectal excision (TME) [13], which requires removal of the entire mesorectum down to the pelvic floor (Fig. 1d). After sufficient intestinal irrigation with saline solution, transection of the rectum was performed using an Echelon™ 60 Endopath stapling device (Ethicon Endo Surgery, Cincinnati, OH, USA) through the additional port, and the specimen was retrieved through the umbilical port. Anastomosis was performed intracorporeally with an EEA circular stapler (Ethicon Endo Surgery) after the anvil was inserted extracorporeally (Fig. 1d). After lavage of the abdominal cavity, a close drain was inserted through the right flank port incision.

C-AR was performed with four to five access ports. Left colonic mobilization, lymph node dissection, high ligation of the inferior mesenteric artery, and anastomosis were performed using techniques similar to those used in the SILS + 1-AR group. In the C-AR group, the umbilical incision was extended for specimen delivery.

Statistical analysis

The Student's t test and Pearson's χ^2 test were used for statistical analyses. All differences were considered significant at $P < 0.05$. All statistical analyses were performed using the Ekuseru-Toukei 2010 software for Windows (Social Survey Research Information Co., Ltd., Tokyo, Japan).

Results

Comparisons between SILS + 1-AR and C-AR

Patient characteristics

The demographic characteristics of the patients in the two groups are presented in Table 1. There were no differences in age, sex, BMI, history of previous surgery, tumor size, stage, or tumor location between the two groups. No patients received preoperative chemoradiotherapy.

Surgical findings

Perioperative results are provided in Table 2. The operating time for SILS + 1-AR was shorter, although not significantly, than that for C-AR (187 [126–308] vs. 222 [139–385] min, $P = 0.062$). There were no significant differences in the mean estimated blood loss (SILS + 1-AR: 22.5 [0–190], C-AR: 34.8 [0–355] mL), number of lymph nodes dissected (SILS + 1-AR: 13.3 ± 7.3, C-AR: 14.5 ± 7.5), number of subserosal invasions (SILS + 1-AR: 12 [60.0 %], C-AR: 9 [45.0 %]), number of lymph node metastases (SILS + 1-AR: 5 [25.0 %], C-AR: 6 [30.0 %]), and the mean length of the distal resection margin (SILS + 1-AR: 32.0 ± 14.4, C-AR: 28.6 ± 14.8 mm). A diverting stoma was utilized in two patients in the SILS + 1-AR group (10.0 %) and two patients in the C-AR group (10.0 %). In the SILS + 1-AR group, no additional ports were placed; however, conversion to open surgery was required in 2 (10 %) of the 20 patients. The reasons for conversion included rectal cancer invasion of the urinary bladder ($n = 1$) and a bulky mass (92 mm) of rectal cancer ($n = 1$). Conversion to open surgery was not required in any of the C-AR patients. All procedures complied with the principles of TME, which requires removal of the entire mesorectum down to the pelvic floor. All cases were circumferential resection margin negative, and the TME was complete with preservation of the bilateral pelvic autonomic nerve. There were no intraoperative complications in either group.

Table 1 Demographics and clinical characteristics of the SILS + 1-AR and C-AR groups

Parameter	SILS + 1-AR ($n = 20$)	C-AR ($n = 20$)	P value
Age (years)	66.4 ± 6.6	68.7 ± 11.1	0.449
Sex			
Male	14	13	1.000
Female	6	7	
BMI (kg/m^2)	23.5 ± 2.9	23.9 ± 3.6	0.673
Operation history (yes/no)	1/19	2/18	1.000
Tumor size (cm)	36.5 ± 21.2	33.8 ± 17.7	0.665
Stage			
0–I	7	8	1.000
II–III	13	12	
Tumor location			
Rs	8	8	1.000
Ra	10	9	
Rb	2	3	

Values are reported as mean (SD) or percentages (%)

Stage and tumor location were determined according to the Japanese Society for Cancer of the Colon and Rectum (JSCCR). The localization of the tumor was categorized as rectosigmoid (Rs), rectum above the peritoneal reflection (Ra), and rectum below the peritoneal reflection (Rb)

BMI body mass index

Table 2 Operative variables in SILS + 1-AR and C-AR groups

Parameter	SILS +1-AR ($n = 20$)	C-AR ($n = 20$)	P value
Operation time (min)	187 (126–308)	222 (139–385)	0.062
Blood loss (mL)	22.5 (0–190)	34.8 (0–355)	0.574
No. of lymph nodes dissected	13.3 ± 7.3	14.5 ± 7.5	0.627
Subserosal invasion (%)	12 (60.0)	9 (45.0)	0.527
Lymph node metastasis (%)	5 (25.0)	6 (30.0)	1.000
Distal resection margin (mm)	32.0 ± 14.4	28.6 ± 14.8	0.466
Adding further port	0 (0.0)	0 (0.0)	1.000
Intraoperative complication	0 (0.0)	0 (0.0)	1.000
Conversion rate (%)	2 (10.0)	0 (0.0)	0.487
Ileostomies (%)	2 (10.0)	2 (10.0)	1.000
Complications	0 (0.0)	0 (0.0)	1.000
Hospital stay (days)	11.3 (7–18)	11.2 (7–23)	0.927

Values are reported as mean (SD) or percentages (%)

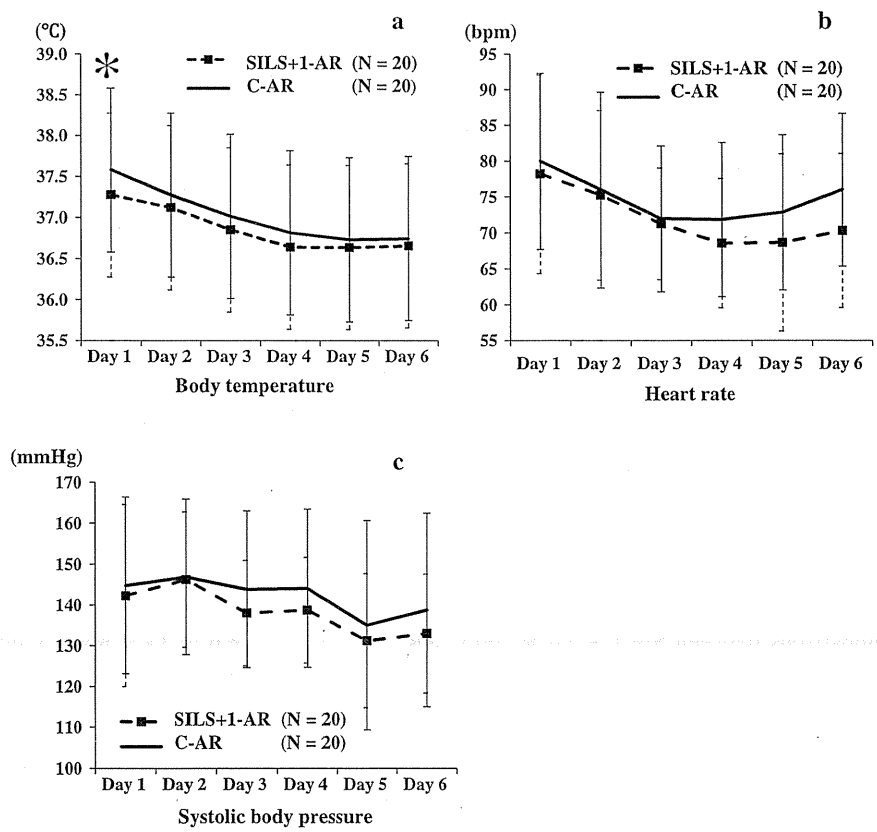

Fig. 2 **a–c** Changes in vital signs after surgery. **a** There was a significant difference in the body temperature in the SILS + 1-AR group on the first postoperative day ($P = 0.028$)

Evaluation of invasiveness

Changes in vital signs

Although the differences were not significant, the SILS + 1-AR group had lower heart rate and systolic blood pressure values after surgery than the C-AR group. A significant difference was observed in the body temperature in the SILS + 1-AR group on POD 1 ($P = 0.028$, Fig. 2).

Changes in hematological parameters

Changes in the hematological parameters are shown in Fig. 3. There were no significant differences in white blood